remote sensing

MDPI

Review

Remote Sensing of Surface and Subsurface Soil Organic Carbon in Tidal Wetlands: A Review and Ideas for Future Research

Rajneesh Sharma [1,*], Deepak R. Mishra [1], Matthew R. Levi [2] and Lori A. Sutter [3]

[1] Department of Geography, University of Georgia, Athens, GA 30602, USA; dmishra@uga.edu
[2] Department of Crop and Soil Sciences, University of Georgia, Athens, GA 30602, USA; matthew.levi@uga.edu
[3] Biology & Marine Biology, University of North Carolina Wilmington, Wilmington, NC 28403, USA; sutterl@uncw.edu
* Correspondence: rajneesh.sharma@uga.edu; Tel.: +1-706-308-9000

Abstract: Tidal wetlands, widely considered the most extensive reservoir of soil organic carbon (SOC), can benefit from remote sensing studies enabling spatiotemporal estimation and mapping of SOC stock. We found that a majority of the remote-sensing-based SOC mapping efforts have been focused on upland ecosystems, not on tidal wetlands. We present a comprehensive review detailing the types of remote sensing models and methods used, standard input variables, results, and limitations for the handful of studies on tidal wetland SOC. Based on that synthesis, we pose several unexplored research questions and methods that are critical for moving tidal wetland SOC science forward. Among these, the applicability of machine learning and deep learning models for predicting surface SOC and the modeling requirements for SOC in subsurface soils (soils without a remote sensing signal, i.e., a soil depth greater than 5 cm) are the most important. We did not find any remote sensing study aimed at modeling subsurface SOC in tidal wetlands. Since tidal wetlands store a significant amount of SOC at greater depths, we hypothesized that surface SOC could be an important covariable along with other biophysical and climate variables for predicting subsurface SOC. Preliminary results using field data from tidal wetlands in the southeastern United States and machine learning model output from mangrove ecosystems in India revealed a strong nonlinear but significant relationship (r^2 = 0.68 and 0.20, respectively, $p < 2.2 \times 10^{-16}$ for both) between surface and subsurface SOC at different depths. We investigated the applicability of the Soil Survey Geographic Database (SSURGO) for tidal wetlands by comparing the data with SOC data from the Smithsonian's Coastal Blue Carbon Network collected during the same decade and found that the SSURGO data consistently over-reported SOC stock in tidal wetlands. We concluded that a novel machine learning framework that utilizes remote sensing data and derived products, the standard covariables reported in the limited literature, and more importantly, other new and potentially informative covariables specific to tidal wetlands such as tidal inundation frequency and height, vegetation species, and soil algal biomass could improve remote-sensing-based tidal wetland SOC studies.

Keywords: belowground soil organic matter; SOC stocks; soil bulk density; Coastal Blue Carbon Network; SSURGO; machine learning; salt marsh; mangroves

Citation: Sharma, R.; Mishra, D.R.; Levi, M.R.; Sutter, L.A. Remote Sensing of Surface and Subsurface Soil Organic Carbon in Tidal Wetlands: A Review and Ideas for Future Research. *Remote Sens.* **2022**, *14*, 2940. https://doi.org/10.3390/rs14122940

Academic Editors: Bas van Wesemael, Sabine Chabrillat, Michael Berger, Adrián Sanz Díaz and Zoltan Szantoi

Received: 3 May 2022
Accepted: 14 June 2022
Published: 20 June 2022

1. Introduction

Wetlands are important transitional ecosystems that remove substantial amounts of nitrogen and phosphorus from upland runoff [1,2]. They play a critical role in recharging water tables, retaining nutrients, absorbing pollutants from runoff, filtering sediment, and sequestering atmospheric carbon [3–6]. Wetlands also support diverse wildlife, fisheries, and wet-field agriculture around the world. Historically, wetlands were considered unproductive agricultural lands. They were often drained and manipulated to allow different agricultural activities to be conducted, but in the late 20th century, the importance of wetlands and ecosystem services was recognized, triggering wide-ranging mapping efforts [1,2]. The early mapping efforts started with identifying the boundaries of wetlands,

vegetation mapping, and periodic surveillance and change detection [7–10]. Due to the rising concentrations of carbon dioxide in the atmosphere, wetlands have become the focus of a wide range of research studies, due to their ability to sequester carbon in large amounts [11]. Wetlands are effective in carbon sequestration due to anaerobic conditions, which lead to the scarcity of oxygen required for efficient carbon decomposition. In the absence of oxygen, less efficient electron acceptors such as Mn and Fe are used for microbially mediated carbon oxidation, and thus organic matter accumulates and is retained for longer durations [12,13]. Wetlands store almost 20–25% of the world's soil organic carbon (SOC) stock in just 4–6% of the world's land area [14]. Recent efforts to evaluate the number of wetlands previously drained have indicated striking losses of wetlands in places such as North America, where wetland loss is estimated to be 53% in the contiguous United States, 16% in Canada, and 62% in Mexico [15,16]. This makes mapping and monitoring changes in SOC in wetlands a critical research area in the broader climate science field. Even though wetlands are a substantial reservoir for longer retention of SOC, the studies on SOC mapping using remote sensing data and techniques have been mainly focused on cropland, grasslands, and forest ecosystems.

We conducted a comprehensive literature review on remote sensing techniques for tidal or coastal wetland SOC prediction and mapping and synthesized our findings, as part of this study. Our objectives for this study were: (1) to provide an in-depth review of existing remote sensing models developed and used to predict SOC in tidal wetlands; (2) to synthesize the standard environmental covariables and propose novel covariables needed to develop accurate, remote-sensing-based SOC prediction models; (3) to analyze the feasibility of modeling subsurface SOC (defined in this review as soils without a remote sensing signal, i.e., a soil depth greater than 5 cm) from remotely estimated surface SOC; and (4) to propose future-facing remote-sensing-based research questions to advance the field of tidal wetland SOC monitoring and mapping. We also include some preliminary data analysis from tidal wetlands in the United States and mangrove wetlands in eastern India, to provide a rationale to support the questions raised as part of future research directions.

2. Past Studies on SOC Modeling and Mapping

2.1. Surface SOC Prediction Modeling across Biomes

Most SOC mapping efforts are based on covariables representing terrain, climate, remotely sensed spectral data, and soil maps, to predict SOC for depths < 50 cm [17]. Predictions with spectral data are commonly limited to surface soils, with most studies focused on a depth of <30 cm. These models primarily use data from hyperspectral and multispectral sensors. For example, data from hyperspectral sensors such as the FieldSpec 4 Hi-Res Spectroradiometer have been used to predict SOC for depths of 0–5 cm [18]. Multispectral sensors such as those of Landsat 8, Sentinel-2, and PlanetScope, and the UAS Parrot Sequoia have been applied to predict SOC for depths of 0–10 cm [19,20]. Hyperspectral sensors are one of the best ways of predicting SOC, due to their better spectral resolution [18], but currently, they are mostly drone-mounted, and data can be expensive to acquire. Multispectral satellite sensors are generally suited for regional-scale and time series SOC mapping [19]. The spatiotemporal coverage of multispectral satellites such as Landsat 1–8 (1972–present) offers a significant advantage in mapping and analyzing the long-term trend in SOC for any given location through a dense time series. Remote-sensing-based SOC mapping studies in terrestrial ecosystems mainly use two approaches depending upon the scale (Table 1). The first approach, at the field scale, uses in situ spectral reflectance and spectral covariables to predict SOC [14,18–21]. At the field scale, the topographic indices derived from lidar sensors are also very commonly used to explain soil variability [22,23]. The second approach, commonly used at regional scales, considers a suite of covariables with or without spectral variables to predict SOC [24–30]. Commonly used spectral covariables in field-scale models include spectral band ratios and reflectance data from red, red-edge, near-infrared (NIR), and shortwave-infrared (SWIR)

wavelengths. Regional-scale models use environmental, climate, topographic, soil type, and land-cover-based covariables. There have been numerous studies on the importance of covariables for terrestrial SOC modeling, and the prediction accuracies of models vary from region to region (Table 1). The prediction accuracy of such models ranges from 35–70%. These studies show that land cover and land use have a significant effect on the SOC stock distribution, which suggests that studying SOC variation within a homogenous type of land cover could yield better results [24,25,27,29,31]. Direct implementation of these terrestrial SOC models in tidal wetlands is not likely to produce accurate results due to the added environmental complexities involving tidal fluctuations, soil saturation with moisture, soil salinity, and the associated vegetation communities [32]. Tidal wetlands also tend to be relatively flat landscapes, which reduces the utility of topographic indices, leaving spectral remote sensing as an obvious predictor for these landscapes [33].

Table 1. Description of common covariables used for SOC predictive models across different SOC mapping studies, their data sources, and their effects on the SOC distribution.

Covariable Type	Common Covariables	Data Source	Common Scale	Literature	Comments
Hyperspectral sensor bands	Visible, Near-infrared, Mid-infrared	Aerial drones, Hyperion on EO-1, PRecursore IperSpettrale della Missione Applicativa (PRISMA), and MightySat II	Usually, field scale, however sensors for regional scales are under development	[18,20,32, 34,35]	Greater accuracy than multispectral data, but limited availability for time series and expensive.
Multispectral sensor bands	Thematic bands, Visible, Near-infrared	Landsat, Sentinel, PlanetScope data, and UAS Parrot Sequoia data	Regional scale and finer	[10,14,19, 25,26,28,31, 32,36–38]	Less accurate than hyperspectral sensors but good for regional scales. Provide continuous data collection for time series analysis.
Vegetation indices	Normalized difference vegetation index (NDVI), Wide dynamic range vegetation index (WDRVI), Soil-adjusted vegetation index (SAVI), Enhanced vegetation index	Sentinel, Landsat, and National Agriculture Imagery Program (NAIP)	Field or regional scales	[11,26,29, 31,38,39]	NDVI is the most commonly used vegetative index, suitable for most study areas. SAVI is a modified vegetation index to adjust for soil pixels. WDRVI and enhanced vegetation index are more site- and need-specific.
Climatic covariables	Normalized moisture index (NDMI), Temperature (mean annual temperature), Precipitation (mean annual precipitation)	Landsat, PRISM database, Worldclim	Field or regional scales	[24,25,27, 28,30,31,36, 39–42]	Temperature and precipitation control other processes such as microbial activity and redox reactions in the soil which further affect SOC.
Topographic factors	Digital elevation model (DEM), Slope, Aspect, Relative slope position, Landform, Topographic wetness index	Numerous	Field or regional scales, depending upon spatial resolution required	[24–31,36,38–40]	DEM-based indices give an idea of uplands and lowlands. Slope dictates the water movement and erosion. The wetness indices represent moisture conditions influenced by topography.
Soil factors	Soil texture, Soil type, Salinity ratio, Drainage classes, Erosional classes, Soil electrical conductivity, Redox potential, etc.	SSURGO, World reference base soils (WRB), Harmonized world soil database, etc.	Regional-scale data from data sources such as SSURGO or STTATGO Field-scale data from sources such as CBCN, NCSS, etc.	[24,26,27, 29,31,38,42, 43]	The proportion of sand and clay in the soil texture can influence the retention of SOC. Various soil types have inherent soil features that dictate horizon thickness, parent material, and major soil processes. Soil salinity can be a very useful covariable in wetland SOC mapping.

2.2. Status of SOC Modeling in Tidal Wetlands

There have been only a limited number of studies on wetland-specific SOC modeling and mapping, due to the scarcity of surface and subsurface SOC data, the lack of bulk den-

sity information, and added challenges regarding water-level fluctuations [44]. Estimating carbon stock is difficult in wetlands because the quantification of net carbon sequestration, the rate of organic matter decomposition, methanogenic micro-organisms, and fluxes from the sediments are complex and hard to isolate [45]. Numerous studies calculate the organic carbon density for subregions and use that to estimate carbon stock across a region [40,46–52]. The calculated SOC is then correlated to available variables from the study area to find the reason for the SOC variability in the region. The main goal of these studies has been to compare carbon stocks between different types of wetlands and find factors or drivers that affect SOC the most. There have been some efforts to predict SOC using a digital soil mapping (DSM) approach in wetlands [6,32,53]. One study used VIS/NIR spectroscopy and EO-1 Hyperion data to compare different machine learning techniques for the estimation of SOC [6]. They concluded that the model using EO-1 Hyperion data and using recursive feature elimination and support vector machine (RF-SVM) gave the best results (r^2 of 0.79 for testing data). Using airborne hyperspectral sensors and spaceborne multispectral sensors such as WorldView-2 and QuickBird to predict soil properties in tidal wetlands showed that prediction accuracy ranged from 0.52 to 0.80, depending upon the data source and modeling techniques [32]. Random forest (RF) and support vector machine (SVM) techniques performed very similarly across the studies [6,32,53]. Other studies used spectral covariables for SOC estimation in tidal wetlands [6,32,33]. Ren et al. [53] used covariables widely applied for SOC mapping in wetlands and found that prediction accuracy reduced with increasing depth. More specifically, they used climatic, remotely sensed, and terrain covariables to predict SOC to a depth of 100 cm, resulting in r^2 values of 0.82, 0.59, and 0.51 for 0–30, 30–60, and 60–100 cm depths, respectively. Zhang et al. [32] suggested that the use of other covariables could increase the prediction accuracy of these models. After reviewing this limited pool of previous studies on remote sensing of wetland SOC, we theorized that using covariables specific to wetland environments along with spectral covariables could increase the prediction accuracy for SOC in these ecosystems.

3. Methods for Wetlands SOC Modeling and Mapping

The covariables used for SOC mapping for wetlands were highly generalized, with no special attention given to the unique environmental factors active in these ecosystems. Most studies on predicting SOC tend to group wetland ecosystems with other ecosystems and predict wetland SOC with the same models used for cropland, grassland, and forest ecosystems [24,27,38]. However, as mentioned earlier, soil composition is greatly influenced by tides, salinity, and the species present in wetlands [32]. Therefore, there is a need to investigate SOC mapping in wetlands independently by exploring the utility of all possible environmental and biophysical covariables. Some models have used the mineral composition of parent materials, environmental factors, topographic factors [24,28,30], and geographic locations from point measurements [29,40]. The choice of covariables for the modeling varies from region to region [24], and the predictive power of a given variable may vary with depth [26,53]. Overall, topographic and climatic variables are the most important for most SOC predictive models [24]. Spectral covariables help to increase the prediction accuracy, and vegetation indices (VIs) such as the normalized difference vegetation index (NDVI) and normalized difference moisture index (NDMI) can be important covariables. In the following section, we discuss the relative importance of covariables for remote-sensing-based wetland SOC modeling.

3.1. Spectral Covariables

Commonly used spectral variables for predicting SOC include reflectance from blue (450–515 nm), green (525–600 nm), red (630–680 nm), near-infrared (NIR) (845–885 nm), and short-wave infrared (SWIR-1) (1560–1660 nm) and SWIR-2 (2100–2300 nm) bands, vegetation indices such as NDVI, and biophysical variables such as NDMI, LAI (leaf area index) and LST (land surface temperature) [6,25,32,53,54]. The most common ways to derive these data are with multispectral (Landsat 8, Sentinel-2, or PlanetScope data, and

UAS Parrot Sequoia data) and hyperspectral sensors (aerial drones, Hyperion on EO-1, and MightySat II).

Zhang et al. [32] found a negative correlation between SOC and spectral reflectance in tidal wetlands in coastal Georgia, United States. The correlation of band wavelengths with SOC varied from r = 0.55 at 932.95 nm to r = 0.34 at 680.5 nm. Ren et al. [53] used spectral covariables such as Landsat visible and SWIR bands, NDVI, LST, LAI, EVI (enhanced vegetation index), NPP (net primary productivity), and LSWI (land surface water index) in the wetlands of western Songnen Plain, China. They reported differences in the importance of spectral covariables for different depths. At 0–30 cm, the covariables with the greatest importance were LST and NDVI, whereas at 30–60 cm, LSWI and LST were the most important and at 60–100 cm, LST and NPP were found to be the most important spectral covariables [53]. Ding et al. [6] also found a negative correlation between spectral reflectance and SOC in the Ebinur Lake wetlands of Xinjiang Uyghur Autonomous Region, China. They observed low reflectance in the visible band (350–780 nm) and high reflectance in the infrared (780–2500 nm). The spectral absorption increased with SOC in the range of 1850–1950 nm, peaking at 2100 nm. They found that a random forest model produced better prediction accuracy than ant colony optimization, interval partial least squares, and recursive feature elimination with support vector machine methods using spectral covariables with an R-value of 0.92 for the test data. Spectral variables are important for SOC mapping because they represent the availability of vegetation biomass in the sensor's field of view (for example, strong Chl—a signal between 650–675 nm wavelength in Figure 1), some of which eventually decomposes and converts into SOC, thus correlating well with the SOC content. One of the challenges of using spectral covariables in wetlands is the lower magnitudes of the reflectances (Figure 1) compared to the upland condition, making it necessary to use more precise sensors to capture minute fluctuations over a relatively small reflectance range. Most wetlands have extensive vegetative cover, and soil property predictions require the ability to connect vegetative community composition from the spectral signatures of the phenology to patterns of soil variability. In addition to spectral patterns, this relationship can also be observed with multi-temporal or hyper-temporal remote sensing [55]. In conclusion, using spectral variables and their derivatives with other environmental, climate, and biophysical covariables would be likely to increase the prediction accuracy of wetland SOC models.

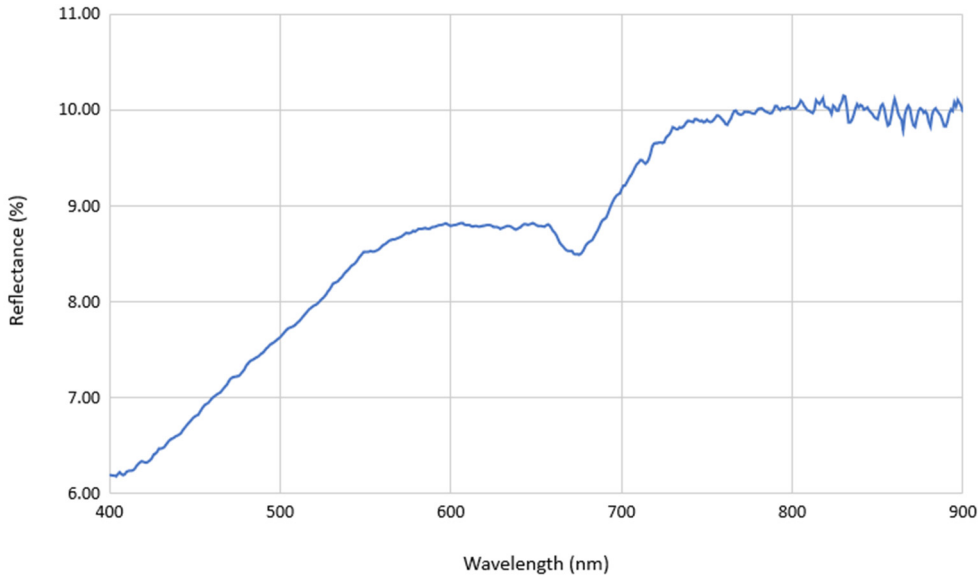

Figure 1. Soil reflectance spectrum using a hyperspectral sensor in tidal wetlands at Sapelo Island, GA. The sensor was a handheld sensor, and the reading was taken with the proximity (approx. 10–15 cm from the soil surface) of soil (Bohicket soil series) under field conditions.

3.2. Climatic Covariables

The most common climatic variables used in existing SOC predictive models are mean annual temperature (MAT) and mean annual precipitation (MAP) [25,40]. Holmquist et al. [50] used climatic zones as one of the covariables to map wetland SOC for the conterminous United States. Usually, the temperature is negatively related to SOC [48,56,57]. Yang (2019) [48] found that temperature significantly affects SOC at greater depths in the tidal wetlands of east central China, whereas Yang et al. (for Tibetan grasslands) [58] and Liu et al. (again for the Tibetan Plateau (northeastern margin of the Qinghai)) [59] found that temperature effects diminished at greater depths. Yang (2019) [48] found the standardized path coefficient between MAT and SOC to be 0.24, using path analysis. Standardized path coefficients are a measure of the effect of MAT on SOC after controlling the other covariable in the model, much like a linear regression model coefficient [60]. Ren et al. (2020) [53] found both MAT (importance factors ~11, 10, and 12 for 0–30, 30–60, and 60–100 cm soil depths, respectively) and MAP (importance factors ~12, 8, and 13 for 0–30, 30–60, and 60–100 cm soil depths) to be in the top five most significant covariables for mapping SOC at all three depths. The prediction accuracy for the SOC model proposed by Han et al. [40] was 76.10%, with the variance explained by MAT (23.74%), latitude (18.2%), longitude (7.12%), and MAP (3.75%). It is important to recognize that climatic variables do not always have predictive power for SOC [33], and the relationships are likely to be influenced by the size and environmental setting of the study area.

The mechanisms of SOC dynamics in wetlands are strongly linked to temperature conditions and water balance. Lower temperatures tend to reduce SOC decomposition and increase the longevity of SOC in wetlands; however, lower temperatures can also lead to lower inputs from net primary productivity [61]. Higher temperatures lead to a reduction in the longevity of SOC due to its more rapid decomposition and conversion to carbon dioxide [62]. The overall impact of temperature on SOC in wetlands can be studied by its effect on inputs and decomposition. SOC content usually increases with higher precipitation, but topographic controls are also important, because landscape position determines the potential for water redistribution and accumulation (e.g., floodplains or tidal wetlands). Higher precipitation creates favorable conditions for biomass production, which leads to eventual decomposition. Latitude is related to tidal amplitude and relative sea-level rise [50]. Tidal amplitude and frequency affect the carbon flux (CO_2 and CH_4 emissions). Tidal amplitude and relative sea-level rise affect the stabilization of SOC in wetlands, and this is discussed thoroughly in later sections. It is also important to recognize that some wetlands can experience drought (i.e., the combined effect of precipitation and temperature), making them susceptible to wildfires, thus further complicating the SOC dynamics [63,64]. Tidal wetlands are climate-sensitive ecosystems, and including climatic covariables in SOC mapping would improve estimation accuracy.

3.3. Topographic Covariables

Variables derived from digital elevation models (DEM) are commonly used for SOC predictive models. For example, slope, aspect, elevation, compound topographic index (CTI), and the System for Automated Geoscientific Analyses (SAGA) wetness index have all been found to be significant predictors in a variety of locations [24,26,27]. Topographic variables capture important patterns of soil erosion and retention of SOC and sediments, making them good predictors of SOC [26].

The relationships of these topographic variables with SOC differ across studies and geographic locations, but one of the most common findings is that low landscape positions tend to have more SOC than high landscape positions. Lower areas tend to be wetter and have more accumulation of organic materials, often concurrently with sediment deposition. For example, the European CTI and SOC were positively correlated, whereas SOC was negatively correlated with elevation and slope [24]. Conversely, Yang et al. [25] found positive relationships of SOC with elevation ($r = 0.31$ and $p = 0.002$) and slope ($r = 0.22$ and $p = 0.026$) and a negative relationship with aspect ($r = -0.36$ and $p < 0.001$) and topographic

wetness index (r = −0.21 and p = 0.024) in an alpine ecosystem on the Tibetan Plateau. Tangen and Bansal [52] found that landscape positions significantly affected SOC, where significant differences (ndf,ddf = 3,1248; F-value = 153.01; p-value < 0.0001) were found in SOC concentrations in the upper 30 cm within upland, toe slope, transition, and inner positions in wetlands of the Prairie Pothole Region of the United States. Wetness index variables such as CTI and the SAGA wetness index are also useful for SOC prediction at depth [26,27]. Ren et al. [53] found elevation to be one of the five most important covariables for all soil depths. They also found that the importance of altitude increased for SOC at greater soil depths (importance factors ~8, 9, and 16 for 0–30, 30–60, and 60–100 cm soil depth, respectively). Han et al. [40] found that altitude explained 15% of the variance and was negatively correlated with SOC in palustrine wetlands in China.

DEM-based covariables such as elevation, slope, relative slope position, and landform are important as they carry information about relative upland or lowland conditions and hence erosional versus depositional areas. Although the variabilities in these factors are expected to be low in tidal wetlands, which are mostly near sea level, they will affect the variability of SOC across depths and are likely to be important covariables for SOC mapping in wetlands. Subtle variations in topography at local and regional scales can have significant impacts on soil property variability and the processes that control SOC dynamics; therefore, detailed DEMs hold great promise for improving predictions of SOC. Given that most wetlands, especially tidal wetlands, have low relief, the best potential for topographic covariables lies in using those from the most detailed digital elevation models (e.g., lidar).

3.4. Soil Covariables

The spatial distribution of other soil properties such as soil types [27,50], soil texture, parent material of soils [28], and soil pH [40] can also be useful for predicting SOC. This concept is recognized in the soil science discipline and has been incorporated conceptually into recent digital soil mapping models [23]. In wetland landscapes, other properties such as soil salinity can be important covariables for SOC mapping [32,50,65].

Holmquist et al. [50] classified soil types into two broad groups, i.e., organic (>13.2%) and inorganic (<13.2%) and found the classification to be the best predictor of SOC (the adjusted effect size (ω^2) for soil type was ~0.8). However, we propose using taxonomy or ecology-based soil classes rather than two broad classes as covariables because of the complex interactions and relationships between environmental variables and soil properties in wetland ecosystems. Soil salinity negatively affects the rate of decomposition of organic matter, due to its effect on SOC organic carbon mineralization [50,65]. We also know that for wet soils, other chemical properties such as pH and the iron and aluminum chemistry affect the stability of SOC [66], and this is unique to soils in and adjacent to wetlands. Han et al. [40] used soil pH to predict SOC, and Macreadie et al. [67] found that soil grain size may also affect SOC [66]. Zhang et al. [32] found a correlation between soil organic matter and soil salinity (r^2 = 0.14). Yang [48] explored the influence of soil properties, including pH, salinity, bulk density, and clay content, on SOC. They found that clay was significantly and positively linked to SOC storage with a standardized path coefficient of 0.68. Bulk density (BD) was also significant in influencing the vertical distribution of SOC, with a standardized coefficient of 0.23. BD is not usually used for predicting SOC stocks in terrestrial ecosystems, due to the interdependency or cross-correlation between both soil properties, but the relationship between BD and SOC in wetlands is unique and is discussed in detail in later sections.

4. Future Directions for Remote-Sensing-Based Tidal Wetland SOC Studies

In this section, we propose and discuss two important hypotheses and future research avenues, including potential open-sourced novel covariables for future research studies focused on remote-sensing-based tidal wetland SOC modeling and mapping. Consolidating

the findings from our literature review, we propose two testable hypotheses for future remote sensing research on wetland SOC estimation and mapping. We hypothesize that:

Hypothesis 1. *Surface SOC is correlated with SOC at depth in tidal wetlands, and the degree of correlation depends on the types of wetlands, depth intervals, species present, environmental factors and gradients, and nature of the active disturbance (natural and anthropogenic) regime.*

Hypothesis 2. *SOC at depth can be predicted using remotely estimated surface SOC in combination with a suite of open-source or satellite-derived biophysical, climatic, and hydrogeomorphic variables for wetlands.*

4.1. Subsurface SOC Estimation in Wetlands

The main limitation for SOC mapping in tidal wetlands has been the inability to predict SOC below the surface layers or subsurface soil due to the limited SOC data at depth. Remote sensing studies that have attempted to predict SOC at depth for tidal wetlands are rare. Köchy et al. [13] mentioned that the scarcity of SOC data at depth leads to a lack of precision in SOC stock estimates in wetlands. Studies such as that of Holmquist et al. [50] had to eliminate numerous SOC point measurements because of the unavailability of data for subsurface soils, which decreased the number of points used for model training from 1959 (0–10 cm SOC point measurements available) to 231 (90–100 cm SOC point measurements available). SOC up to a depth of 0–15 cm is commonly predicted by remote sensing techniques with reasonable accuracy and can be used to gain valuable insights into agricultural systems. However, significant amounts of SOC reside in subsurface soils in wetlands (Table 2), and surface SOC captures only a small proportion of the overall SOC stock. The unique saturated conditions in wetlands enable soils to capture and retain SOC in surface and subsurface layers for a long period. Ren et al. [53] make one of the rare efforts to try to predict SOC within 0–100 cm in wetlands (Western Songnen Plain, China), but the predictive power of the used covariables decreased three-fold from 0.72 r^2 (SOC at 0–30 cm) to 0.25 r^2 (SOC at 60–100 cm), when the inverse distance weighting technique was used. SOC does not vary in the same way with depth in tidal wetlands as in other land covers. In almost all land covers except wetlands, SOC reduces with depth; however, in wetlands and other soils affected by high water tables, it can even increase with depth, at least up to certain depths [68]. Although the SOC distribution across depth in wetlands has been well recognized by several studies, SOC stock prediction studies have not attempted to predict SOC for subsurface soils.

Table 2. Comparison between Coastal Blue Carbon Network data and SSURGO data for the southeastern coastal United States for various soil depths using Wilcoxon matched pairs signed exact test for non-parametric datasets.

SOC Depths	CBCN Data (kg/m^2)	SSURGO (kg/m^2)	95% Confidence Interval (kg/m^2)	*p*-Value
0–5 cm	1.5	3.3	1.4–2.4	4.77×10^{-9}
5–20 cm	4.6	9.4	3.5–6.3	7.19×10^{-9}
20–50 cm	8	14.8	3.5–9.6	1.36×10^{-5}
50–100 cm	11.1	20.6	3.8–15.4	1.81×10^{-3}
100–150 cm	16.4	17.5	(−15.1)–22	0.43

We propose that future remote-sensing-based wetland SOC estimation models should focus on both surface SOC and subsurface SOC. Remote sensing data may carry some information about surface SOC depending on the wetland vegetation density and canopy structure. Therefore, remote-sensing-based empirical, semi-analytical, or data-centric models can be used directly to estimate surface SOC. Although limited, there have been remote sensing studies (discussed here previously) that have demonstrated success in mapping surface SOC in wetlands. Remote sensing data, however, do not contain any signals from

subsurface soil. To estimate SOC at depths, one can utilize machine learning (ML) or deep learning (DL) models with all possible biophysical, climatic, and hydrogeomorphic covariables, which might carry some information on SOC at depth by reflecting the spatial patterns of soil properties and important processes that control SOC variability. In that scenario, surface estimates of SOC would be one of the most important covariables, assuming there is a significant correlation between surface and subsurface SOC in wetlands. This is very similar to the soil prediction model introduced by McBratney et al. [23], which proposed the use of existing or attainable soil property information as a complement to other common predictors, for improving estimates of desired soil properties. Consequently, accurate prediction of surface SOC is crucial for subsurface SOC modeling. One caveat is that such data-centric modeling would require extensive training datasets, representing a wide range of wetland types, species, and conditions, with all possible covariables and with ground-truth soil core data acquired coincidentally. That is not a trivial effort. To the best of our knowledge, such a comprehensive dataset either does not exist or must be derived or put together piecemeal if it does exist for certain well-studied sites. In the absence of such a dataset, using limited available ground-truth and model output data, in the following sections we have provided our rationale and preliminary results justifying the scientific basis behind these hypotheses regarding future research directions for remote sensing studies focused on wetland SOC modeling and mapping.

4.2. Relation between Surface and Subsurface SOC in Wetlands: A Case Study

In this section, we present a research case study demonstrating the relationship between surface and subsurface SOC. Since remote sensing studies on subsurface SOC are nonexistent, through the presentation of this case study we aim to provide preliminary results as a justification for our Hypothesis 1. To test Hypothesis 1, we examined the relationship between surface SOC (0–5 cm) and SOC at depth by using SOC data from two sources: first, model output from a mangrove wetland site in eastern India and second, field measurements from tidal wetlands in the southeastern United States.

Method: The mangrove SOC data were obtained from efforts in India and contain model outputs covering approximately 2400 pixels (496 m) from Bhitarkanika National Park, India (Figure 2) [69,70]. This is a Ramsar site (one of the 2424 internationally important wetland sites recognized by UNESCO) located in the eastern state of Odisha in India, covering 145 sq. km of mangrove forests [71]. The model explained 89%, 85%, 79%, 77%, 76%, and 67% of the variability of the training data for soil depths of 0–5 cm, 5–15 cm, 15–30 cm, 30–60 cm, 60–100 cm, and 100–200 cm, respectively, with RMSE values ranging from 0.23–0.32 and explained 33%, 30%, 20%, 17%, 14%, and 10% of the variability for the validation data for soil depths in same order with RMSE values ranging from 0.1–0.33. The SOC data for tidal wetlands in the southeastern United States were retrieved from the Coastal Blue Carbon Network (CBCN) database maintained by the Smithsonian Environmental Research Center (SERC), Edgewater, Maryland, United States. The dataset consisted of 262 point locations for the southeastern tidal wetlands of the United States, and the data were collected between 2007 and 2018 (Figure 3). The CBCN database is a data consortium for wetland SOC point measurements from various research studies in the coastal areas of the United States [50,72–108]. Studies contributing to the CBCN database follow the National Wetland Condition Assessment guidelines for field sampling [72].

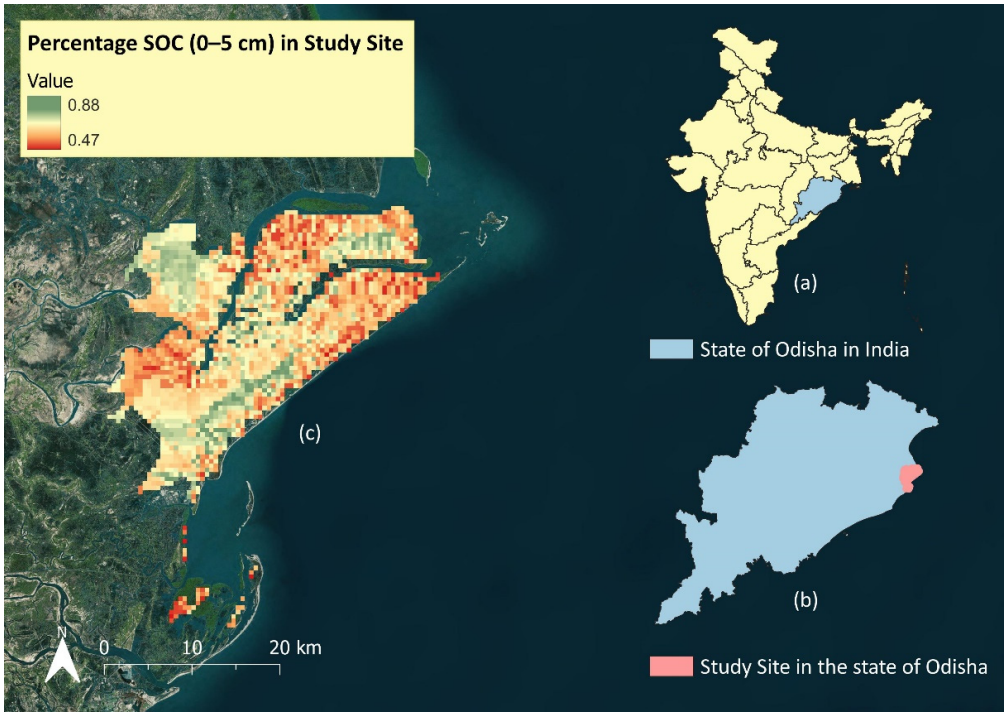

Figure 2. Study locations starting top right and moving clockwise: (**a**) the state of Odisha, India; (**b**) Bhitarkanika National Park in Odisha, India; (**c**) distribution of SOC in upper 5 cm of the soil surface in mangrove wetlands of Bhitarkanika National Park, Odisha, India.

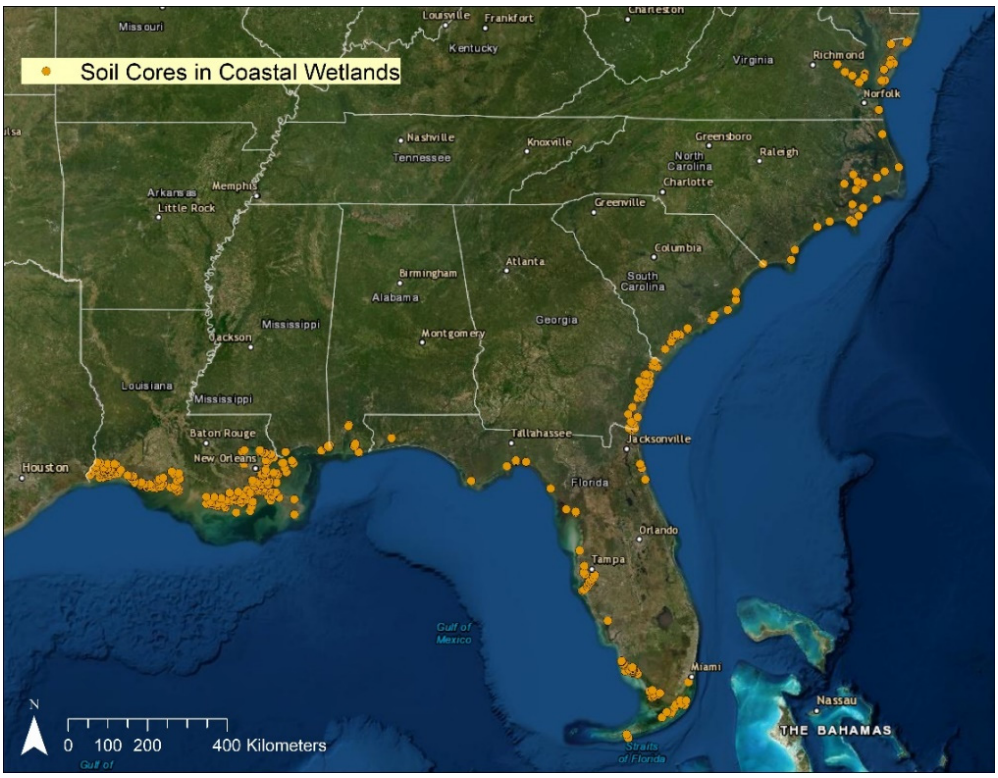

Figure 3. Distribution of 261 point locations of SOC measurements in the southeastern coastal United States. These points, collected between 2007 and 2018, were retrieved from the Coastal Blue Carbon Network (CBCN) database.

SOC data from both the datasets were standardized for specified depths using the AQP package in R, where 0–5 cm represented the soil surface and 5–15 cm, 15–30 cm, 30–60 cm, 60–100 cm, and 100–200 cm depths were considered subsurface depths. For the mangrove SOC data from India, all 2400 pixels had modeled SOC data for all SOC depths; however, the number of points having SOC data for various depths differed for the CBCN database. A total of 261 points for the surface (0–5 cm) had data. Comparison between surface and subsurface SOC was constrained by SOC data from subsurface depths. A total of 248 points from 5–15 cm, 244 points from 15–30 cm, 185 points from 30–60 cm, 106 points from 60–100 cm, and 52 points from 100–200 cm were used for the comparison. As the SOC data were positively skewed or non-parametric, the correlations between surface and subsurface depths were computed using the Spearman's rank correlation rho coefficient [109] (called the Spearman's coefficient from now on). The correlation coefficients between surface (0–5 cm) and subsurface depths are shown in Figure 4.

Results and Discussion: Our initial analysis using the SOC data from the mangrove site in Bhitarkanika National Park, India and the United States tidal wetlands showed that surface SOC was significantly correlated with SOC at depth up to a certain depth. The correlation generally decreased with depth (Figure 4), and there was no relationship below 60 cm soil depth for the Indian mangrove site. However, the correlation between surface SOC (0–5 cm) and SOC in the whole soil pedon (0–200 cm) was also significant ($p < 2.2 \times 10^{-16}$), with a Spearman's coefficient of 0.20 for the mangrove site and 0.68 for the United States tidal wetlands. Although this result is preliminary, it supports our hypotheses that a correlation between surface and subsurface SOC exists in wetlands and the strength of the correlation is dependent on species, site, and a host of active covariables. The Spearman's coefficients for the Indian mangroves and United States salt marshes were notably different from each other for the same depth ranges (Figure 4). We propose some possible explanations for these differences in the strength of the correlation between surface and subsurface SOC. First, the nature of the correlation varies based on wetland types, which would support our hypotheses. Second, SOC data from the southeastern coastal United States tidal wetlands were derived from soil cores taken in the field, so these can be treated as verifiable ground-truth data. SOC data from the Indian mangrove site, in contrast, were model outputs from a deep learning model, and there was greater uncertainty (10–30% uncertainty for different depths based on Lin's concordance correlation between predicted and actual SOC concentrations for training data) associated with the model [70]. This would need further field investigation to verify. However, examining the results obtained in this analysis, surface SOC was more strongly correlated to SOC at depth in the tidal wetlands of the United States than in the mangrove wetlands studied in India. Tidal wetlands observed in the United States are mainly salt marshes, and wetlands evaluated in the Bhitarkanika region of India are completely dominated by mangroves [110]. Mangroves store a greater C density deeper in the profile (e.g., 30–60 cm) due to their root structure, in contrast to marshes where the majority of roots are closer to the surface [111]. Additionally, predicting SOC in mangroves carries a standard error almost twice as large as in salt marshes [112] and, perhaps because of their unique carbon-storing mechanism, there are differences between surface and subsurface SOC. This could explain the relatively lower correlation of surface SOC observed in mangroves compared to salt marshes.

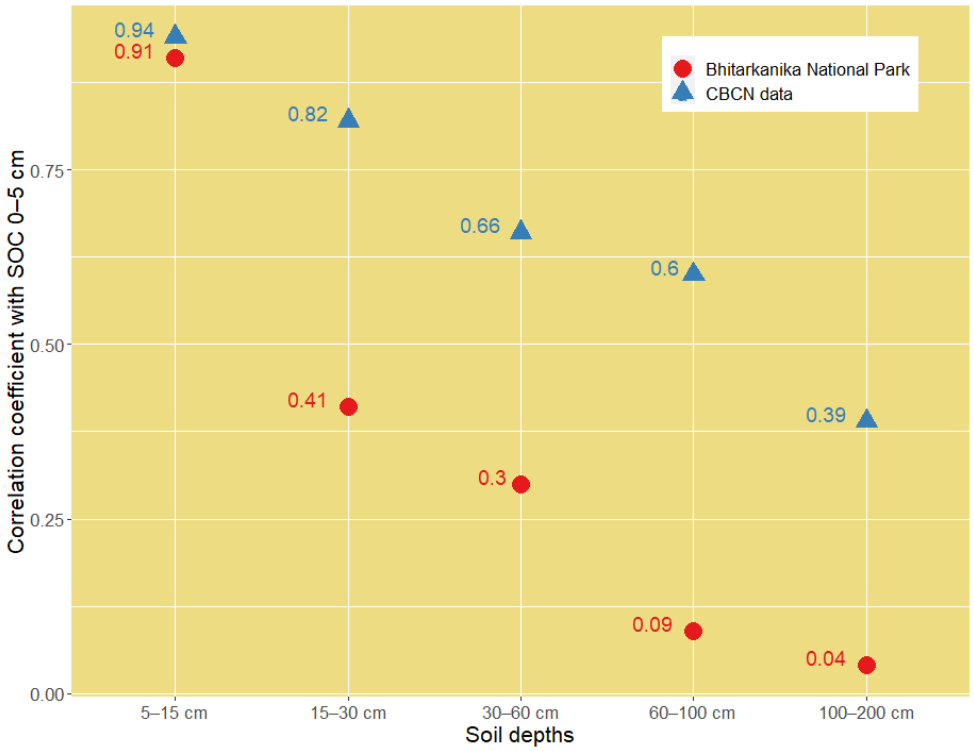

Figure 4. The Spearman's coefficients between surface SOC percent (0–5 cm) and SOC percent in various depths of soil for the tidal wetlands in the southeastern coastal United States (shown in blue) and mangrove wetlands in the Odisha state of India (shown in orange) [69,113]. Data for Bhitarkanika National Park mangrove site were used with permission from Chakraborty et al. [69].

4.3. Comparison of SSURGO Data with CBCN Database

We also compared the Soil Survey Geographic Database (SSURGO) distributed by the Natural Resources Conservation Service (NRCS) [114] with the CBCN database for the southeastern coastal United States wetlands. Our goal was to determine whether the SSURGO data could be used with the SOC point database to generate extra training data to be used in a future ML or DL modeling frameworks for predicting SOC distribution in wetlands. Point data from the CBCN database were used to extract the *mukey* (SSURGO polygon ID) from gridded SSURGO, also known as gSSURGO (raster version of SSURGO data with pixel size 10 m). The mukey extracted from gSSURGO was used to connect data points to the SSURGO database for obtaining SOC stock measurements. A total of 261 CBCN database SOC points (Figure 3) were spread across 100 gSSURGO clusters with a unique mukey. The SOC values from the CBCN database were averaged for points with an identical mukey to make the comparison. The SOC data from the CBCN database were standardized for depths (Table 2) to match the SSURGO SOC data. The SOC data from both sources were neither normal nor non-parametric, and SOC data represent the same mukey (SSURGO polygon). Therefore, a paired Wilcoxon matched pairs signed exact test [115] was used. Unlike Zhong and Xu [116], who observed a weak positive correlation between organic matter reported in the SSURGO dataset and independently collected soil cores from tidal wetlands in Louisiana, United States, we found that SOC values from SSURGO data and CBCN data were significantly different from each other (except at the 100–150 cm depth; Table 2). SSURGO data were mostly extracted in 2018, with some data from 2007, whereas CBCN data were from 2007–2018 with most data points from 2011, followed by points from 2017–2018. SSURGO data consistently yielded higher SOC stocks compared to CBCN data for different depth ranges, as reported in Table 2. The inconsistencies between the two data types could be due to temporal differences or (most probably) the scale differences between the datasets. SSURGO records averaged SOC values for each soil map

unit, whereas Coastal Blue Carbon Network data are point-based data. The density of CBCN points was not the same for each SSURGO polygon, creating a spatial scale mismatch which, according to us, is the major reason for the mismatch in SOC values between the two datasets, given that there were not enough point data for each SSURGO polygon to make a comprehensive comparison. Another reason for the higher SOC stock prediction by SSURGO data than by CBCN data could be the lack of accurate bulk density data for tidal wetlands, and the bulk density values listed in the SSURGO database could be higher for organic-rich tidal wetland soils. We conclude that the SSURGO database can be used in conjunction with other point data if soil map-unit-based SOC stock predictions are needed; however, the scale and methodology of data collection for the two datasets should be given proper thought. Since NRCS is presently expanding its data collection in coastal and marine environments, this will remain another avenue for future research [117].

4.4. Remote-Sensing-Based Subsurface SOC Prediction Model Framework with Standard and Proposed Novel Covariables

For Hypothesis 2, we developed an expanded set of standard and novel covariables that could be used in a future data-centric modeling framework. The uniqueness of the wetland ecosystem allows for the usage of some potentially novel covariables or wetland-specific environmental, climatic, and hydrogeomorphic drivers for SOC modeling and mapping that have not been explored or fully utilized in the existing studies. The covariables provided in Table 1 have been well studied and can be used to explain SOC stock variability in wetlands. For example, Holmquist et al. [50] used covariables such as climate zones (based on the EPA's greenhouse gas inventory), salinity, vegetation, and soil classes in their study and concluded that these variables together were not sufficient for predicting carbon density in wetlands. There is a need for studies exploring additional wetland-specific covariables, especially covariables derived from spectral remote sensing [33]. We developed a modeling framework that integrates techniques commonly used in the SOC modeling literature with a suite of covariables we believe are important for wetlands (Figure 5). We grouped the standard and proposed novel covariables separately as a list of input variables to be considered in future wetland SOC modeling studies. All listed covariables can either be remotely sensed, derived from remote sensing data, or are already available in open-source databases, which is an important consideration to ensure the broad applicability of these models to sites where field data are lacking or collection is not possible.

Vegetation plays an important role in providing biomass for SOC [32]. Yang [48] discussed how a single invasive species *Sporobolus alterniflorus* (formerly *Spartina alterniflora*) increased the SOC storage by 0.0078 kg m^{-2} per year ($r^2 = 0.66$ and $p < 0.001$) at a depth of 0–30 cm and 0.134 kg m^{-2} per year ($r^2 = 0.29$ and $p < 0.05$) at a depth of 0–100 cm in the tidal wetlands of China where it was introduced. Holmquist et al. [50] also recognized vegetation species as a significant covariable affecting SOC in wetlands in the conterminous United States. Most studies use NDVI, which is a vegetation index with some information about aboveground biomass that eventually gets converted into SOC. Although not a great proxy for biomass, NDVI may provide an idea about the source of SOC. However, it fails to capture the biogeochemical effects that vegetation type has on gross production and regulation of SOC in wetlands. Therefore, a vegetation species map could be an important covariable along with traditional vegetation indices for SOC predictions in wetlands. A vegetation species map can be derived using high-resolution open-source satellite data such as Sentinel-2 (10 m) or Planet (3 m) datasets. Vegetation can also be a good indicator of soil differences, which might also affect SOC throughout the profile.

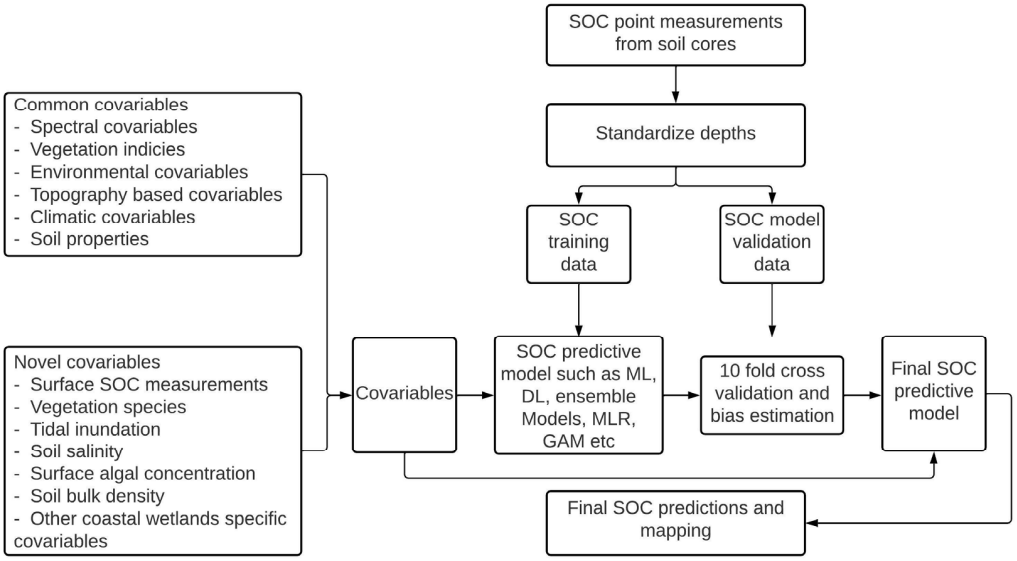

Figure 5. Model diagram for the suggested subsurface SOC modeling technique in wetland ecosystems (ML: machine learning; DL: deep learning; MLR: multiple linear regression; GAM: generalized additive models).

As well as vegetation species, it might also be useful to consider biogeochemical processes, which are controlled by microbial and fungal communities in wetlands. Pei et al. [118] found that arbuscular mycorrhizal fungi (AMF) affected the carbon sequestration in wetlands in the northeast region of China. Remote sensing of AMF is a very new research field with some initial effort (e.g., [119]). Biotic factors such as AMF with a signal emitting potential can be used as a potential covariable for SOC modeling. Soil algal content, with soil chlorophyll-a as a proxy, is another such biotic covariable that can increase the predictability of SOC modeling in wetlands. Algae tracking is not only important for the environment but can also be related to SOC variability across wetlands. Algal concentration has a large impact on light penetration and controls other environmental factors that can affect SOC. The surface algae in wetlands can potentially influence the soil properties and the microbial activities that affect SOC. Algal concentration as a covariable has not been explored in any SOC modeling studies to the best of our knowledge, but there have been some recent efforts to estimate algal concentrations using remote sensing techniques [120,121].

Soil bulk density (BD) as a covariable could be uniquely used in wetlands. Numerous studies have explained the effect of SOC on BD, but in wetlands, SOC might have a complex relationship with BD, and thus BD could be a covariable for predicting SOC in wetlands. In wetlands, BD is affected by tidal inundation and sediment deposition rather than just plant root growth [122]. BD affects the stabilization of both surface and subsurface carbon in tidal wetlands [48]. However, the use of bulk density must be checked for bias, as SOC percent and bulk density are both used to obtain SOC stock-per-unit-area values, and the usage of bulk density in the model can create a bias in predicting SOC stock. Additionally, field measurements of bulk density are scarce, and most of the machine learning models used to predict BD use SOC as covariables. There are some recent efforts to develop predictive models for wetland soil bulk density using remote sensing, with accuracies ranging from 50–88% [123–125].

Other important covariables in wetland SOC modeling are tidal inundation (magnitude and extent) and soil salinity. Tides in marine wetlands control soil salinity, algal deposition, vegetative species, decomposition of SOC, and microbial activities. The amplitude and frequency of tides control the spatial distribution of soil salinity that affects CO_2 and CH_4 emission fluxes [4,32,126]. Mueller et al. [127] found a 29% reduction in the stabilization of organic matter in frequently flooded areas compared to less frequently flooded areas. Wang et al. [128] found that increasing marsh salinity from 6 to 9 ppt resulted

in 50–80% more CO_2 emissions and typically decreased CH_4 emissions, whereas decreasing marsh salinity from 26 to 19 ppt did not affect CO_2 and CH_4 emissions. Tidal inundation detection models have already been developed using remote sensing data. For example, the Tidal Marsh Inundation Index (TMII) was developed, which implements MODIS (250 m) images in the salt marsh ecosystems of Georgia and the United States Gulf Coast [129]. Similarly, a model (Flooding in Landsat Across Tidal Systems (FLATS)) has been developed to detect flooding using Landsat (30 m) images in a salt marsh ecosystem [130].

5. Conclusions

Tidal wetland ecosystems are unique, highly diverse, and effective sequesters of atmospheric carbon. SOC modeling studies using remote sensing techniques in tidal wetlands are surprisingly scarce. We conclude that SOC mapping techniques used for other ecosystems need to be modified when applied to tidal wetlands, and tidal wetland-specific covariables should be incorporated into the list of standard covariables to capture the diversity and unique environmental conditions. We found a significant correlation between surface SOC and SOC at various depths up to 2 m, but the strength of this correlation varied across soil depths and approached 0 below a 60 cm soil depth for the Bhitarkanika mangroves. However, based on the significant correlation between surface SOC and SOC in the whole soil pedon (0–200 cm), we conclude that the relationship between surface and subsurface SOC can be used in subsurface SOC modeling studies in tidal wetlands. However, this is one of many covariables which, when used in combination, could enhance the final modeling outcome. The strength of the final model will be dependent upon wetland type, depth interval, vegetative species, and other environmental factors. Vegetation species and tidal inundation are underutilized in SOC modeling and mapping studies, but they could be important factors affecting SOC distribution in tidal wetlands. The uniqueness of tidal wetlands allows the exploration of other less commonly used covariables that could be significant for tidal wetland SOC studies. For example, soil algae distribution should be explored further as a potential covariable. The development of accurate SOC models using remote-sensing-data-based machine learning or deep learning techniques will advance SOC mapping in tidal wetlands in the near future. Developing a machine learning or deep learning model based on remotely sensed data from legacy satellite sensors such as the Landsat series, MODIS, VIIRS, or AVHRR would provide us with a multi-decadal time-series trend for SOC distribution in many tidal wetlands. Collectively, this powerful dataset could be used to answer various unexplored questions related to wetland carbon dynamics and the role of tidal wetlands in the global blue carbon budget, such as:

- What are the spatiotemporal trends in tidal wetland soil carbon dynamics over the past 50 years?
- How does climate change impact the carbon-storing capacity of wetlands?
- What other factors (such as vegetation and soil properties) control the distribution of carbon in wetlands in space and time?
- What are the impacts of the press (sea level rise, increasing atmospheric CO_2) vs. pulse (hurricanes, flash droughts, freshwater fluxes associated with extreme precipitation events) disturbances on wetland SOC?

There is a significant gap in the research and a clear need for remote-sensing-based modeling studies on tidal wetland SOC mapping. Tidal wetlands cannot be treated the same way as terrestrial ecosystems and need to be given special attention in SOC prediction and mapping. Remote-sensing-based modeling techniques could be the only viable method of large-scale spatiotemporal mapping of surface and at-depth SOC in tidal wetlands.

Author Contributions: R.S. conceptualized the study and processed and analyzed the data; R.S. and D.R.M. wrote and edited different parts of the manuscript; D.R.M., M.R.L. and L.A.S. reviewed, edited, and provided supervision; and R.S. produced the visualization. All authors have read and agreed to the published version of the manuscript.

Funding: This study was supported by NSF and USDA's Signals in the Soil (SitS) program, under grant award number 2021-67019-34342, and by the USDA and NRCS cooperative agreement NR1874820006C003.

Data Availability Statement: Not applicable.

Acknowledgments: We would like to thank the Department of Geography at the University of Georgia for providing funding to the graduate student involved in this research. The authors would like to thank Bhabani Das of the Indian Institute of Technology, Kharagpur, India and a co-author of the studies Chakraborty et al. (2020) and Reddy et al. (2020) for providing data and model outputs for mangrove ecosystems in eastern India. We would also like to thank the Smithsonian Environmental Research Center's Coastal Blue Carbon Network and the US Department of Agriculture (USDA) Natural Resources Conservation Service (NRCS) for the wetland soils data.

Conflicts of Interest: The authors declare no conflict of interest.

References

1. Rundquist, D.C.; Narumalani, S.; Narayanan, R.M. A Review of Wetlands Remote Sensing and Defining New Considerations. *Remote Sens. Rev.* **2001**, *20*, 207–226. [CrossRef]
2. Mitsch, W.J.; Gosselink, W.J.G. *Wetlands*; John Wiley & Sons: Hoboken, NJ, USA, 2015.
3. Dugan, P. (Ed.) *Wetlands in Danger: A World Conservation Atlas*; Introduction by David Bellamy; Oxford University Press: New York, NY, USA, 1993; ISBN 0195209427.
4. Luo, M.; Huang, J.F.; Zhu, W.F.; Tong, C. Impacts of Increasing Salinity and Inundation on Rates and Pathways of Organic Carbon Mineralization in Tidal Wetlands: A Review. *Hydrobiologia* **2019**, *827*, 31–49. [CrossRef]
5. Barbier, E.B.; Hacker, S.D.; Kennedy, C.; Koch, E.W.; Stier, A.C.; Silliman, B.R. The Value of Estuarine and Coastal Ecosystem Services. *Ecol. Monogr.* **2011**, *81*, 169–193. [CrossRef]
6. Ding, J.; Yang, A.; Wang, J.; Sagan, V.; Yu, D. Machine-Learning-Based Quantitative Estimation of Soil Organic Carbon Content by VIS/NIR Spectroscopy. *PeerJ* **2018**, *6*, e5714. [CrossRef]
7. Reimold, R.J.; Gallagher, J.L.; Thompson, D.E. Coastal Mapping with Remote Sensors. In *Proceedings of the Coastal Mapping Symposium*; American Society of Photogrammetry: Washington, DC, USA, 1972; pp. 99–112.
8. Anderson, R.R.; Carter, V.L.; Mcginness, J.W., Jr. Mapping Southern Atlantic Coastal Marshland, South Carolina-Georgia, Using ERTS-1 Imagery; NASA Technical Reports Server (NTRS). 1973. Available online: https://ntrs.nasa.gov/citations/19730010631 (accessed on 24 January 2021).
9. Dahl, T.E. *Wetlands Losses in the United States 1780's to 1980's*; U.S. Department of the Interior, Fish and Wild Life Service: Washington, DC, UDA, 1990; 13p. Available online: https://www.fws.gov/wetlands/documents/Wetlands-Losses-in-the-United-States-1780s-to-1980s.pdf (accessed on 12 October 2021).
10. Hardisky, M.A.; Gross, M.F.; Klemas, V. Remote Sensing of Coastal Wetlands. *BioScience* **1986**, *36*, 453–460. [CrossRef]
11. Byrd, K.B.; Ballanti, L.; Thomas, N.; Nguyen, D.; Holmquist, J.R.; Simard, M.; Windham-Myers, L. A Remote Sensing-Based Model of Tidal Marsh Aboveground Carbon Stocks for the Conterminous United States. *ISPRS J. Photogramm. Remote Sens.* **2018**, *139*, 255–271. [CrossRef]
12. Freeman, C.; Ostle, N.; Kang, H. An Enzymic "latch" on a Global Carbon Store. *Nature* **2001**, *409*, 149. [CrossRef]
13. Köchy, M.; Hiederer, R.; Freibauer, A. Global Distribution of Soil Organic Carbon—Part 1: Masses and Frequency Distributions of SOC Stocks for the Tropics, Permafrost Regions, Wetlands, and the World. *Soil* **2015**, *1*, 351–365. [CrossRef]
14. Yu, J.; Wang, Y.; Li, Y.; Dong, H.; Zhou, D.; Han, G.; Wu, H.; Wang, G.; Mao, P.; Gao, Y. Soil Organic Carbon Storage Changes in Coastal Wetlands of the Modern Yellow River Delta from 2000 to 2009. *Biogeosci. Discuss.* **2012**, *9*, 1759–1779. [CrossRef]
15. Shrestha, G.; Cavallaro, N.; Lorenzoni, L.; Seadler, A.; Zhu, Z.; Gurwick, N.P.; Larson, E.; Birdsey, R.; Mayes, M.A.; Najjar, R.G.; et al. Highlights. In *Second State of the Carbon Cycle Report (SOCCR2): A Sustained Assessment Report*; Cavallaro, N., Shrestha, G., Birdsey, R., Mayes, M.A., Najjar, R.G., Reed, S.C., Romero-Lankao, P., Zhu, Z., Eds.; U.S. Global Change Research Program: Washington, DC, USA, 2018; pp. 1–4. [CrossRef]
16. Kolka, R.; Trettin, C.; Tang, W.; Krauss, K.; Bansal, S.; Drexler, J.; Wickland, K.; Chimner, R.; Hogan, D.; Pindilli, E.J.; et al. Chapter 13: Terrestrial wetlands. In *Second State of the Carbon Cycle Report (SOCCR2): A Sustained Assessment Report*; Cavallaro, N., Shrestha, G., Birdsey, R., Mayes, M.A., Najjar, R.G., Reed, S.C., Romero-Lankao, P., Zhu, Z., Eds.; U.S. Global Change Research Program: Washington, DC, USA, 2018; pp. 507–567. [CrossRef]
17. Minasny, B.; McBratney, A.B.; Malone, B.P.; Wheeler, I. Digital Mapping of Soil Carbon. *Adv. Agron.* **2013**, *118*, 1–47. [CrossRef]
18. Shen, L.; Gao, M.; Yan, J.; Li, Z.L.; Leng, P.; Yang, Q.; Duan, S.B. Hyperspectral Estimation of Soil Organic Matter Content Using Different Spectral Preprocessing Techniques and PLSR Method. *Remote Sens.* **2020**, *12*, 1206. [CrossRef]
19. Žížala, D.; Minarík, R.; Zádorová, T. Soil Organic Carbon Mapping Using Multispectral Remote Sensing Data: Prediction Ability of Data with Different Spatial and Spectral Resolutions. *Remote Sens.* **2019**, *11*, 2947. [CrossRef]
20. Dvorakova, K.; Shi, P.; Limbourg, Q.; van Wesemael, B. Soil Organic Carbon Mapping from Remote Sensing: The Effect of Crop Residues. *Remote Sens.* **2020**, *12*, 1913. [CrossRef]

21. Nawar, S.; Munnaf, M.A.; Mouazen, A.M. Machine Learning Based On-Line Prediction of Soil Organic Carbon after Removal of Soil Moisture Effect. *Remote Sens.* **2020**, *12*, 1308. [CrossRef]
22. Maleki, S.; Khormali, F.; Mohammadi, J.; Bogaert, P.; Bagheri Bodaghabadi, M. Effect of the Accuracy of Topographic Data on Improving Digital Soil Mapping Predictions with Limited Soil Data: An Application to the Iranian Loess Plateau. *Catena* **2020**, *195*, 104810. [CrossRef]
23. McBratney, A.B.; Mendonça Santos, M.L.; Minasny, B. On Digital Soil Mapping. *Geoderma* **2003**, *117*, 3–52. [CrossRef]
24. Aksoy, E.; Yigini, Y.; Montanarella, L. Combining Soil Databases for Topsoil Organic Carbon Mapping in Europe. *PLoS ONE* **2016**, *11*, e0152098. [CrossRef]
25. Yang, R.M.; Zhang, G.L.; Liu, F.; Lu, Y.Y.; Yang, F.; Yang, F.; Yang, M.; Zhao, Y.G.; Li, D.C. Comparison of Boosted Regression Tree and Random Forest Models for Mapping Topsoil Organic Carbon Concentration in an Alpine Ecosystem. *Ecol. Indic.* **2016**, *60*, 870–878. [CrossRef]
26. Taghizadeh-Mehrjardi, R.; Nabiollahi, K.; Kerry, R. Digital Mapping of Soil Organic Carbon at Multiple Depths Using Different Data Mining Techniques in Baneh Region, Iran. *Geoderma* **2016**, *266*, 98–110. [CrossRef]
27. Adhikari, K.; Hartemink, A.E.; Minasny, B.; Bou Kheir, R.; Greve, M.B.; Greve, M.H. Digital Mapping of Soil Organic Carbon Contents and Stocks in Denmark. *PLoS ONE* **2014**, *9*, e105519. [CrossRef]
28. Grinand, C.; Maire, G.L.; Vieilledent, G.; Razakamanarivo, H.; Razafimbelo, T.; Bernoux, M. Estimating Temporal Changes in Soil Carbon Stocks at Ecoregional Scale in Madagascar Using Remote-Sensing. *Int. J. Appl. Earth Obs. Geoinf.* **2017**, *54*, 1–14. [CrossRef]
29. Hamzehpour, N.; Shafizadeh-Moghadam, H.; Valavi, R. Exploring the Driving Forces and Digital Mapping of Soil Organic Carbon Using Remote Sensing and Soil Texture. *Catena* **2019**, *182*, 104141. [CrossRef]
30. Wang, B.; Waters, C.; Orgill, S.; Gray, J.; Cowie, A.; Clark, A.; Liu, D.L. High Resolution Mapping of Soil Organic Carbon Stocks Using Remote Sensing Variables in the Semi-Arid Rangelands of Eastern Australia. *Sci. Total Environ.* **2018**, *630*, 367–378. [CrossRef] [PubMed]
31. Schillaci, C.; Acutis, M.; Lombardo, L.; Lipani, A.; Fantappiè, M.; Märker, M.; Saia, S. Spatio-Temporal Topsoil Organic Carbon Mapping of a Semi-Arid Mediterranean Region: The Role of Land Use, Soil Texture, Topographic Indices and the Influence of Remote Sensing Data to Modelling. *Sci. Total Environ.* **2017**, *601–602*, 821–832. [CrossRef]
32. Zhang, C.; Mishra, D.R.; Pennings, S.C. Mapping Salt Marsh Soil Properties Using Imaging Spectroscopy. *ISPRS J. Photogramm. Remote Sens.* **2019**, *148*, 221–234. [CrossRef]
33. Wang, S.; Zhou, M.; Zhuang, Q.; Guo, L. Prediction Potential of Remote Sensing-Related Variables in the Topsoil Organic Carbon Density of Liaohekou Coastal Wetlands, Northeast China. *Remote Sens.* **2021**, *13*, 4106. [CrossRef]
34. Gomez, C.; Viscarra Rossel, R.A.; McBratney, A.B. Soil Organic Carbon Prediction by Hyperspectral Remote Sensing and Field Vis-NIR Spectroscopy: An Australian Case Study. *Geoderma* **2008**, *146*, 403–411. [CrossRef]
35. PRISMA Data Are Now Available for Access—Surface Biology and Geology. Available online: https://sbg.jpl.nasa.gov/news-events/prisma-data-are-now-available-for-access (accessed on 1 June 2022).
36. Somarathna, P.D.S.N.; Malone, B.P.; Minasny, B. Mapping Soil Organic Carbon Content over New South Wales, Australia Using Local Regression Kriging. *Geoderma Reg.* **2016**, *7*, 38–48. [CrossRef]
37. Castaldi, F.; Chabrillat, S.; Don, A.; van Wesemael, B. Soil Organic Carbon Mapping Using LUCAS Topsoil Database and Sentinel-2 Data: An Approach to Reduce Soil Moisture and Crop Residue Effects. *Remote Sens.* **2019**, *11*, 2121. [CrossRef]
38. Kempen, B.; Dalsgaard, S.; Kaaya, A.K.; Chamuya, N.; Ruipérez-González, M.; Pekkarinen, A.; Walsh, M.G. Mapping Topsoil Organic Carbon Concentrations and Stocks for Tanzania. *Geoderma* **2019**, *337*, 164–180. [CrossRef]
39. Samdandorj, M.; Ts, P. Geospatial Modeling Approaches for Mapping Topsoil Organic Carbon Stock in Northern Part of Mongolia. *Proc. Mong. Acad. Sci.* **2019**, *59*, 4–17. [CrossRef]
40. Han, L.; Wan, Z.; Guo, Y.; Song, C.; Jin, S.; Zuo, Y. Estimation of Soil Organic Carbon Storage in Palustrine Wetlands, China. *Int. J. Environ. Res. Public Health* **2020**, *17*, 4646. [CrossRef] [PubMed]
41. Yigini, Y.; Panagos, P. Assessment of Soil Organic Carbon Stocks under Future Climate and Land Cover Changes in Europe. *Sci. Total Environ.* **2016**, *557–558*, 838–850. [CrossRef] [PubMed]
42. Osland, M.J.; Gabler, C.A.; Grace, J.B.; Day, R.H.; McCoy, M.L.; McLeod, J.L.; From, A.S.; Enwright, N.M.; Feher, L.C.; Stagg, C.L.; et al. Climate and Plant Controls on Soil Organic Matter in Coastal Wetlands. *Glob. Chang. Biol.* **2018**, *24*, 5361–5379. [CrossRef] [PubMed]
43. FAO. *FAO Global Soil Organic Carbon Map (GSOCmap)*; FAO: Rome, Italy, 2018; ISBN 978-92-5-130439-6. Available online: http://www.fao.org/documents/card/en/c/I8891EN (accessed on 12 February 2022).
44. Tidal Wetland Soil Carbon Stocks for the Conterminous United States, 2006–2010. Available online: https://daac.ornl.gov/cgi-bin/dsviewer.pl?ds_id=1612 (accessed on 7 November 2021).
45. Mitra, S.; Wassmann, R.; Vlek, P.L.G. An Appraisal of Global Wetland Area and Its Organic Carbon Stock. *Curr. Sci.* **2005**, *88*, 25–35.
46. Hinson, A.L.; Feagin, R.A.; Eriksson, M.; Najjar, R.G.; Herrmann, M.; Bianchi, T.S.; Kemp, M.; Hutchings, J.A.; Crooks, S.; Boutton, T. The Spatial Distribution of Soil Organic Carbon in Tidal Wetland Soils of the Continental United States. *Glob. Chang. Biol.* **2017**, *23*, 5468–5480. [CrossRef]
47. Xu, S.; Liu, X.; Li, X.; Tian, C. Soil Organic Carbon Changes Following Wetland Restoration: A Global Meta-Analysis. *Geoderma* **2019**, *353*, 89–96. [CrossRef]

48. Yang, R.M. Interacting Effects of Plant Invasion, Climate, and Soils on Soil Organic Carbon Storage in Coastal Wetlands. *J. Geophys. Res. Biogeosci.* **2019**, *124*, 2554–2564. [CrossRef]
49. Jinbo, Z.; Changchun, S.; Shenmin, W. Dynamics of Soil Organic Carbon and Its Fractions after Abandonment of Cultivated Wetlands in Northeast China. *Soil Tillage Res.* **2007**, *96*, 350–360. [CrossRef]
50. Holmquist, J.R.; Windham-Myers, L.; Bliss, N.; Crooks, S.; Morris, J.T.; Megonigal, J.P.; Troxler, T.; Weller, D.; Callaway, J.; Drexler, J.; et al. Accuracy and Precision of Tidal Wetland Soil Carbon Mapping in the Conterminous United States. *Sci. Rep.* **2018**, *8*, 9478. [CrossRef]
51. Bernal, B.; Mitsch, W.J. A Comparison of Soil Carbon Pools and Profiles in Wetlands in Costa Rica and Ohio. *Ecol. Eng.* **2008**, *34*, 311–323. [CrossRef]
52. Tangen, B.A.; Bansal, S. Soil Organic Carbon Stocks and Sequestration Rates of Inland, Freshwater Wetlands: Sources of Variability and Uncertainty. *Sci. Total Environ.* **2020**, *749*, 141444. [CrossRef] [PubMed]
53. Ren, Y.; Li, X.; Mao, D.; Wang, Z.; Jia, M.; Chen, L. Investigating Spatial and Vertical Patterns of Wetland Soil Organic Carbon Concentrations in China's Western Songnen Plain by Comparing Different Algorithms. *Sustainability* **2020**, *12*, 932. [CrossRef]
54. Peng, Y.; Xiong, X.; Adhikari, K.; Knadel, M.; Grunwald, S.; Greve, M.H. Modeling Soil Organic Carbon at Regional Scale by Combining Multi-Spectral Images with Laboratory Spectra. *PLoS ONE* **2015**, *10*, e0142295. [CrossRef]
55. Maynard, J.J.; Levi, M.R. Hyper-Temporal Remote Sensing for Digital Soil Mapping: Characterizing Soil-Vegetation Response to Climatic Variability. *Geoderma* **2017**, *285*, 94–109. [CrossRef]
56. Albaladejo, J.; Ortiz, R.; Garcia-Franco, N.; Navarro, A.R.; Almagro, M.; Pintado, J.G.; Martínez-Mena, M. Land Use and Climate Change Impacts on Soil Organic Carbon Stocks in Semi-Arid Spain. *J. Soils Sediments* **2013**, *13*, 265–277. [CrossRef]
57. Jobba´gy, E.G.; Jobba´gy, J.; Jackson, R.B. *April 2000 423 Belowground Processes and Global Change 423 the Vertical Distribution of Soil Organic Carbon and Its Relation to Climate and Vegetation*; John Wiley & Sons, Ltd.: Hoboken, NJ, USA, 2000; Volume 10.
58. Yang, Y.H.; Fang, J.Y.; Guo, D.L.; Ji, C.J.; Ma, W.H. Vertical Patterns of Soil Carbon, Nitrogen and Carbon: Nitrogen Stoichiometry in Tibetan Grasslands. *Biogeosci. Discuss.* **2010**, *7*, 1–24. [CrossRef]
59. Liu, W.; Chen, S.; Qin, X.; Baumann, F.; Scholten, T.; Zhou, Z.; Sun, W.; Zhang, T.; Ren, J.; Qin, D. Storage, Patterns, and Control of Soil Organic Carbon and Nitrogen in the Northeastern Margin of the Qinghai-Tibetan Plateau. *Environ. Res. Lett.* **2012**, *7*, 035401. [CrossRef]
60. Lleras, C. Path Analysis. In *Encyclopedia of Social Measurement*; Elsevier: New York, NY, USA, 2005; Volume 3, pp. 25–30. Available online: https://www.researchgate.net/profile/Paul-Louangrath/post/Can_anybody_clearly_define_differences_between_Path_analysis_and_error_in_regression_analysis/attachment/59d63b74c49f478072ea7410/AS%3A273741995544576%401442276585356/download/Path_Analysis.pdf (accessed on 11 November 2021).
61. Davidson, E.A.; Trumbore, S.E.; Amundson, R. Soil Warming and Organic Carbon Content. *Nature* **2000**, *408*, 789–790. [CrossRef]
62. Bonneville, M.C.; Strachan, I.B.; Humphreys, E.R.; Roulet, N.T. Net Ecosystem CO2 Exchange in a Temperate Cattail Marsh in Relation to Biophysical Properties. *Agric. For. Meteorol.* **2008**, *148*, 69–81. [CrossRef]
63. Watts, A.C. Organic Soil Combustion in Cypress Swamps: Moisture Effects and Landscape Implications for Carbon Release. *For. Ecol. Manag.* **2013**, *294*, 178–187. [CrossRef]
64. Watts, A.C.; Kobziar, L.N. Smoldering Combustion and Ground Fires: Ecological Effects and Multi-Scale Significance. *Fire Ecol.* **2013**, *9*, 124–132. [CrossRef]
65. Qu, W.; Li, J.; Han, G.; Wu, H.; Song, W.; Zhang, X. Effect of Salinity on the Decomposition of Soil Organic Carbon in a Tidal Wetland. *J. Soils Sediments* **2019**, *19*, 609–617. [CrossRef]
66. Rasmussen, C.; Heckman, K.; Wieder, W.R.; Keiluweit, M.; Lawrence, C.R.; Berhe, A.A.; Blankinship, J.C.; Crow, S.E.; Druhan, J.L.; Hicks Pries, C.E.; et al. Beyond Clay: Towards an Improved Set of Variables for Predicting Soil Organic Matter Content. *Biogeochemistry* **2018**, *137*, 297–306. [CrossRef]
67. Macreadie, P.I.; Ollivier, Q.R.; Kelleway, J.J.; Serrano, O.; Carnell, P.E.; Ewers Lewis, C.J.; Atwood, T.B.; Sanderman, J.; Baldock, J.; Connolly, R.M.; et al. Carbon Sequestration by Australian Tidal Marshes. *Sci. Rep.* **2017**, *7*, srep44071. [CrossRef]
68. Bai, J.; Zhang, G.; Zhao, Q.; Lu, Q.; Jia, J.; Cui, B.; Liu, X. Depth-Distribution Patterns and Control of Soil Organic Carbon in Coastal Salt Marshes with Different Plant Covers. *Sci. Rep.* **2016**, *6*, 34835. [CrossRef]
69. Chakraborty, P.; Das, B.S.; Vasava, H.B.; Panigrahi, N.; Santra, P. Spatial Structure, Parameter Nonlinearity, and Intelligent Algorithms in Constructing Pedotransfer Functions from Large-Scale Soil Legacy Data. *Sci. Rep.* **2020**, *10*, 15050. [CrossRef]
70. Reddy, N.N.; Chakraborty, P.; Roy, S.; Singh, K.; Minasny, B.; McBratney, A.B.; Biswas, A.; Das, B.S. Legacy Data-Based National-Scale Digital Mapping of Key Soil Properties in India. *Geoderma* **2020**, *381*, 114684. [CrossRef]
71. Rasquinha, D.N.; Mishra, D.R. Impact of Wood Harvesting on Mangrove Forest Structure, Composition and Biomass Dynamics in India. *Estuar. Coast. Shelf Sci.* **2021**, *248*, 106974. [CrossRef]
72. Nahlik, A.M.; Fennessy, M.S. Carbon Storage in US Wetlands. *Nat. Commun.* **2016**, *7*, 13835. [CrossRef]
73. Craft, C. Freshwater Input Structures Soil Properties, Vertical Accretion, and Nutrient Accumulation of Georgia and U.S. Tidal Marshes. *Limnol. Oceanogr.* **2007**, *52*, 1220–1230. [CrossRef]
74. Spivak, A.C.; Canuel, E.A.; Duffy, J.E.; Douglass, J.G.; Richardson, J.P. Epifaunal Community Composition and Nutrient Addition Alter Sediment Organic Matter Composition in a Natural Eelgrass Zostera Marina Bed: A Field Experiment. *Mar. Ecol. Prog. Ser.* **2009**, *376*, 55–67. [CrossRef]

75. Neubauer, S.C.; Anderson, I.C.; Constantine, J.A.; Kuehl, S.A. Sediment Deposition and Accretion in a Mid-Atlantic (U.S.A.) Tidal Freshwater Marsh. *Estuar. Coast. Shelf Sci.* **2002**, *54*, 713–727. [CrossRef]
76. McGlathery, K.J.; Reynolds, L.K.; Cole, L.W.; Orth, R.J.; Marion, S.R.; Schwarzschild, A. Recovery Trajectories during State Change from Bare Sediment to Eelgrass Dominance. *Mar. Ecol. Prog. Ser.* **2012**, *448*, 209–221. [CrossRef]
77. Buzzelli, C.P. Dynamic Simulation of Littoral Zone Habitats in Lower Chesapeake Bay. I. Ecosystem Characterization Related to Model Development. *Estuaries* **1998**, *21*, 659–672. [CrossRef]
78. Noe, G.B.; Hupp, C.R.; Bernhardt, C.E.; Krauss, K.W. Contemporary Deposition and Long-Term Accumulation of Sediment and Nutrients by Tidal Freshwater Forested Wetlands Impacted by Sea Level Rise. *Estuaries Coasts* **2016**, *39*, 1006–1019. [CrossRef]
79. Jones, M.C.; Bernhardt, C.E.; Krauss, K.W.; Noe, G.B. The Impact of Late Holocene Land Use Change, Climate Variability, and Sea Level Rise on Carbon Storage in Tidal Freshwater Wetlands on the Southeastern United States Coastal Plain. *J. Geophys. Res. Biogeosci.* **2017**, *122*, 3126–3141. [CrossRef]
80. Krauss, K.W.; Noe, G.B.; Duberstein, J.A.; Conner, W.H.; Stagg, C.L.; Cormier, N.; Jones, M.C.; Bernhardt, C.E.; Graeme Lockaby, B.; From, A.S.; et al. The Role of the Upper Tidal Estuary in Wetland Blue Carbon Storage and Flux. *Glob. Biogeochem. Cycles* **2018**, *32*, 817–839. [CrossRef]
81. Drexler, J.Z.; Krauss, K.W.; Sasser, M.C.; Fuller, C.C.; Swarzenski, C.M.; Powell, A.; Swanson, K.M.; Orlando, J. A Long-Term Comparison of Carbon Sequestration Rates in Impounded and Naturally Tidal Freshwater Marshes along the Lower Waccamaw River, South Carolina. *Wetlands* **2013**, *33*, 965–974. [CrossRef]
82. Townsend, E.C.; Fonseca, M.S. Bioturbation as a Potential Mechanism Influencing Spatial Heterogeneity of North Carolina Seagrass Beds. *Mar. Ecol. Prog. Ser.* **1998**, *169*, 123–132. [CrossRef]
83. Fourqurean, J.W.; Duarte, C.M.; Kennedy, H.; Marbà, N.; Holmer, M.; Mateo, M.A.; Apostolaki, E.T.; Kendrick, G.A.; Krause-Jensen, D.; McGlathery, K.J.; et al. Seagrass Ecosystems as a Globally Significant Carbon Stock. *Nat. Geosci.* **2012**, *5*, 505–509. [CrossRef]
84. Smith, K.E.L.; Flocks, J.G.; Steyer, G.D.; Piazza, S.C. *Wetland Paleoecological Study of Southwest Coastal Louisiana: Sediment Cores and Diatom Calibration Dataset*; Data Series 877; U.S. Geological Survey: Reston, VA, USA, 2015. [CrossRef]
85. Piazza, S.C.; Steyer, G.D.; Cretini, K.F.; Sasser, C.E.; Visser, J.M.; Holm, G.O.; Sharp, L.A.; Evers, D.E.; Meriwether, J.R. *Geomorphic and Ecological Effects of Hurricanes Katrina and Rita on Coastal Louisiana Marsh Communities*; Open-File Report 2011-1094; U.S. Geological Survey: Reston, VA, USA, 2011; pp. i–126. [CrossRef]
86. Nymanl, J.A.; Delaunel, R.D.; Patrick, W.H., Jr. Relationship between Vegetation and Soil Formation in a Rapidly Submerging Coastal Marsh. *Mar. Ecol. Prog. Ser.* **1993**, *96*, 269–279. [CrossRef]
87. Abbott, K.M.; Elsey-Quirk, T.; DeLaune, R.D. Factors Influencing Blue Carbon Accumulation across a 32-Year Chronosequence of Created Coastal Marshes. *Ecosphere* **2019**, *10*, e02828. [CrossRef]
88. Rosenfeld, J.K. Interstitial Water and Sediment Chemistry of Two Cores from Florida Bay. *J. Sediment. Res.* **1979**, *49*, 989–994. [CrossRef]
89. Yarbro, L.A.; Carlson, P.R. Community Oxygen and Nutrient Fluxes in Seagrass Beds of Florida Bay, USA. *Estuaries Coasts* **2008**, *31*, 877–897. [CrossRef]
90. Yando, E.S.; Osland, M.J.; Willis, J.M.; Day, R.H.; Krauss, K.W.; Hester, M.W. Salt Marsh-Mangrove Ecotones: Using Structural Gradients to Investigate the Effects of Woody Plant Encroachment on Plant–Soil Interactions and Ecosystem Carbon Pools. *J. Ecol.* **2016**, *104*, 1020–1031. [CrossRef]
91. Smoak, J.M.; Breithaupt, J.L.; Smith, T.J.; Sanders, C.J. Sediment Accretion and Organic Carbon Burial Relative to Sea-Level Rise and Storm Events in Two Mangrove Forests in Everglades National Park. *Catena* **2013**, *104*, 58–66. [CrossRef]
92. Radabaugh, K.R.; Moyer, R.P.; Chappel, A.R.; Powell, C.E.; Bociu, I.; Clark, B.C.; Smoak, J.M. Coastal Blue Carbon Assessment of Mangroves, Salt Marshes, and Salt Barrens in Tampa Bay, Florida, USA. *Estuaries Coasts* **2018**, *41*, 1496–1510. [CrossRef]
93. Osland, M.J.; Grace, J.B.; Stagg, C.L.; Day, R.H.; Hartley, S.B.; Enwright, N.M.; Gabler, C.A. *U.S. Gulf of Mexico Coast (TX, MS, AL, and FL) Vegetation, Soil, and Landscape Data (2013–2014)*; U.S. Geological Survey: Reston, VA, USA, 2016. [CrossRef]
94. Osland, M.J.; Spivak, A.C.; Nestlerode, J.A.; Lessmann, J.M.; Almario, A.E.; Heitmuller, P.T.; Russell, M.J.; Krauss, K.W.; Alvarez, F.; Dantin, D.D.; et al. Ecosystem Development after Mangrove Wetland Creation: Plant-Soil Change across a 20-Year Chronosequence. *Ecosystems* **2012**, *15*, 848–866. [CrossRef]
95. Geochemistry of Florida Bay Sediments: Nutrient History at Five Sites in Eastern and Central Florida Bay on JSTOR. Available online: https://www.jstor.org/stable/4299024?seq=1 (accessed on 3 June 2022).
96. Marchio, D.A.; Savarese, M.; Bovard, B.; Mitsch, W.J. Carbon Sequestration and Sedimentation in Mangrove Swamps Influenced by Hydrogeomorphic Conditions and Urbanization in Southwest Florida. *Forests* **2016**, *7*, 116. [CrossRef]
97. Lewis, M.A.; Dantin, D.D.; Chancy, C.A.; Abel, K.C.; Lewis, C.G. Florida Seagrass Habitat Evaluation: A Comparative Survey for Chemical Quality. *Environ. Pollut.* **2007**, *146*, 206–218. [CrossRef] [PubMed]
98. Grady, J.R. Properties of Sea Grass and Sand Flat Sediments from the Intertidal Zone of St. Andrew Bay, Florida. *Estuaries* **1981**, *4*, 335–344. [CrossRef]
99. Gerlach, M.J.; Engelhart, S.E.; Kemp, A.C.; Moyer, R.P.; Smoak, J.M.; Bernhardt, C.E.; Cahill, N. Reconstructing Common Era Relative Sea-Level Change on the Gulf Coast of Florida. *Mar. Geol.* **2017**, *390*, 254–269. [CrossRef]
100. Fourqurean, J.W.; Muth, M.F.; Boyer, J.N. Epiphyte Loads on Seagrasses and Microphytobenthos Abundance Are Not Reliable Indicators of Nutrient Availability in Oligotrophic Coastal Ecosystems. *Mar. Pollut. Bull.* **2010**, *60*, 971–983. [CrossRef]

101. Doughty, C.L.; Langley, J.A.; Walker, W.S.; Feller, I.C.; Schaub, R.; Chapman, S.K. Mangrove Range Expansion Rapidly Increases Coastal Wetland Carbon Storage. *Estuaries Coasts* **2016**, *39*, 385–396. [CrossRef]
102. Chmura, G.L.; Anisfeld, S.C.; Cahoon, D.R.; Lynch, J.C. Global Carbon Sequestration in Tidal, Saline Wetland Soils. *Glob. Biogeochem. Cycles* **2003**, *17*, 1111. [CrossRef]
103. Chen, R.; Twilley, R.R. A Simulation Model of Organic Matter and Nutrient Accumulation in Mangrove Wetland Soils. *Biogeochemistry* **1999**, *44*, 93–118. [CrossRef]
104. Sanderman, J.; Hengl, T.; Fiske, G.; Solvik, K.; Adame, M.F.; Benson, L.; Bukoski, J.J.; Carnell, P.; Cifuentes-Jara, M.; Donato, D.; et al. A Global Map of Mangrove Forest Soil Carbon at 30 m Spatial Resolution. *Environ. Res. Lett.* **2018**, *13*, 055002. [CrossRef]
105. BURNS, S.J.; SWART, P.K. Diagenetic Processes in Holocene Carbonate Sediments: Florida Bay Mudbanks and Islands. *Sedimentology* **1992**, *39*, 285–304. [CrossRef]
106. Breithaupt, J.L.; Smoak, J.M.; Rivera-Monroy, V.H.; Castañeda-Moya, E.; Moyer, R.P.; Simard, M.; Sanders, C.J. Partitioning the Relative Contributions of Organic Matter and Mineral Sediment to Accretion Rates in Carbonate Platform Mangrove Soils. *Mar. Geol.* **2017**, *390*, 170–180. [CrossRef]
107. Arriola, J.M.; Cable, J.E. Variations in Carbon Burial and Sediment Accretion along a Tidal Creek in a Florida Salt Marsh. *Limnol. Oceanogr.* **2017**, *62*, S15–S28. [CrossRef]
108. Noe, G.B.; Krauss, K.W.; Lockaby, B.G.; Conner, W.H.; Hupp, C.R. The Effect of Increasing Salinity and Forest Mortality on Soil Nitrogen and Phosphorus Mineralization in Tidal Freshwater Forested Wetlands. *Biogeochemistry* **2013**, *114*, 225–244. [CrossRef]
109. Hauke, J.; Kossowski, T. Repozytorium Uniwersytetu Im. Adama Mickiewicza (AMUR): Comparison of Values of Pearson's and Spearman's Correlation Coefficient on the Same Sets of Data. Available online: https://repozytorium.amu.edu.pl/handle/10593/15580 (accessed on 31 January 2022).
110. Banerjee, K.; Bal, G.; Mitra, A. How Soil Texture Affects the Organic Carbon Load in the Mangrove Ecosystem? A Case Study from Bhitarkanika, Odisha. In *Environmental Pollution*; Springer: Singapore, 2018; pp. 329–341. [CrossRef]
111. Meng, W.; Feagin, R.A.; Hu, B.; He, M.; Li, H. The Spatial Distribution of Blue Carbon in the Coastal Wetlands of China. *Estuarine Coast. Shelf Sci.* **2019**, *222*, 13–20. [CrossRef]
112. Alongi, D.M. Carbon Balance in Salt Marsh and Mangrove Ecosystems: A Global Synthesis. *J. Mar. Sci. Eng.* **2020**, *8*, 767. [CrossRef]
113. Data Clearinghouse | Smithsonian Environmental Research Center. Available online: https://serc.si.edu/coastalcarbon/data (accessed on 18 January 2021).
114. Soil Survey Staff, Natural Resources Conservation Service, U.S. Soil Survey Staff, Natural Resources Conservation Service, United States Department of Agriculture. Soil Survey Geographic (SSURGO) Database. Available online: https://Sdmdataaccess.Sc.Egov.Usda.Gov (accessed on 31 January 2021).
115. Woolson, R.F. Wilcoxon Signed-Rank Test. In *Wiley Encyclopedia of Clinical Trials*; John Wiley & Sons, Inc.: Hoboken, NJ, USA, 2007; pp. 1–3. [CrossRef]
116. Zhong, B.; Xu, Y.J. Scale Effects of Geographical Soil Datasets on Soil Carbon Estimation in Louisiana, USA: A Comparison of STATSGO and SSURGO. *Pedosphere* **2011**, *21*, 491–501. [CrossRef]
117. Soil Survey Technical Note 12 | NRCS Soils. Available online: https://www.nrcs.usda.gov/wps/portal/nrcs/detail/soils/ref/?cid=nrcseprd1469015 (accessed on 21 October 2021).
118. Pei, L.; Ye, S.; Yuan, H.; Pei, S.; Xie, S.; Wang, J. Glomalin-Related Soil Protein Distributions in the Wetlands of the Liaohe Delta, Northeast China: Implications for Carbon Sequestration and Mineral Weathering of Coastal Wetlands. *Limnol. Oceanogr.* **2019**, *65*, 979–991. [CrossRef]
119. Fisher, J.B.; Sweeney, S.; Brzostek, E.R.; Evans, T.P.; Johnson, D.J.; Myers, J.A.; Bourg, N.A.; Wolf, A.T.; Howe, R.W.; Phillips, R.P. Tree-Mycorrhizal Associations Detected Remotely from Canopy Spectral Properties. *Glob. Chang. Biol.* **2016**, *22*, 2596–2607. [CrossRef]
120. Papenfus, M.; Schaeffer, B.; Pollard, A.I.; Loftin, K. Exploring the Potential Value of Satellite Remote Sensing to Monitor Chlorophyll-a for US Lakes and Reservoirs. *Environ. Monit. Assess.* **2020**, *192*, 808. [CrossRef]
121. Sebastiá-Frasquet, M.T.; Aguilar-Maldonado, J.A.; Herrero-Durá, I.; Santamaría-Del-ángel, E.; Morell-Monzó, S.; Estornell, J. Advances in the Monitoring of Algal Blooms by Remote Sensing: A Bibliometric Analysis. *Appl. Sci.* **2020**, *10*, 7877. [CrossRef]
122. Wang, H.; Piazza, S.C.; Sharp, L.A.; Stagg, C.L.; Couvillion, B.R.; Steyer, G.D.; McGinnis, T.E. Determining the Spatial Variability of Wetland Soil Bulk Density, Organic Matter, and the Conversion Factor between Organic Matter and Organic Carbon across Coastal Louisiana, USA. *J. Coast. Res.* **2017**, *33*, 507–517. [CrossRef]
123. Pittman, R.; Hu, B. Estimation of soil bulk density and carbon using multi-source remotely sensed data. *ISPRS Ann. Photogramm. Remote Sens. Spat. Inf. Sci.* **2020**, *5*, 541–548. [CrossRef]
124. Aitkenhead, M.; Coull, M. Mapping Soil Profile Depth, Bulk Density and Carbon Stock in Scotland Using Remote Sensing and Spatial Covariates. *Eur. J. Soil Sci.* **2020**, *71*, 553–567. [CrossRef]
125. Hikouei, I.S.; Kim, S.S.; Mishra, D.R. Machine-Learning Classification of Soil Bulk Density in Salt Marsh Environments. *Sensors* **2021**, *21*, 4408. [CrossRef] [PubMed]
126. Bradley, P.M.; Morris, J.T. The Influence of Salinity on the Kinetics of NHinf4sup+ Uptake in Spartina Alterniflora. *Oecologia* **1991**, *85*, 375–380. [CrossRef] [PubMed]

127. Mueller, P.; Schile-Beers, L.M.; Mozdzer, T.J.; Chmura, G.L.; Dinter, T.; Kuzyakov, Y.; de Groot, A.V.; Esselink, P.; Smit, C.; D'Alpaos, A.; et al. Global-Change Effects on Early-Stage Decomposition Processes in Tidal Wetlands-Implications from a Global Survey Using Standardized Litter. *Biogeosciences* **2018**, *15*, 3189–3202. [CrossRef]
128. Wang, F.; Kroeger, K.D.; Gonneea, M.E.; Pohlman, J.W.; Tang, J. Water Salinity and Inundation Control Soil Carbon Decomposition during Salt Marsh Restoration: An Incubation Experiment. *Ecol. Evol.* **2019**, *9*, 1911–1921. [CrossRef]
129. O'Connell, J.L.; Mishra, D.R.; Cotten, D.L.; Wang, L.; Alber, M. The Tidal Marsh Inundation Index (TMII): An Inundation Filter to Flag Flooded Pixels and Improve MODIS Tidal Marsh Vegetation Time-Series Analysis. *Remote Sens. Environ.* **2017**, *201*, 34–46. [CrossRef]
130. Narron, C.R.; O'Connell, J.L.; Mishra, D.R.; Cotten, D.L.; Hawman, P.A.; Mao, L. Flooding in Landsat across Tidal Systems (FLATS): An index for intermittent tidal filtering and frequency detection in salt marsh environments. *Ecol. Indic.* 2022; *in press*.